Design and Synthesis of a New Class of Selective Integrin α5β1 Antagonists

Roland Stragies,* Frank Osterkamp, Gunther Zischinsky, Doerte Vossmeyer, Holger Kalkhof, Ulf Reimer, and Grit Zahn

Jerini AG, Invalidenstrasse 130, Berlin, D-10115 Germany

Received January 2, 2007

Starting from the structure of integrin αvβ3 in a complex with a peptidic ligand plus SAR data on nonpeptidic ligands, we derived a new class of integrin α5β1 antagonists (**1**). Several synthesis strategies were applied to evaluate the chemical space around the essential pharmacophore groups R_1 to R_3 to obtain highly active and selective pyrrolidine derivatives as integrin α5β1 antagonists. Integrin selectivity was controlled by switching from a sulfonamide moiety to a mesitylene amide moiety for R_3. This finding represents a general feature for modulating selectivity toward other related integrin receptors. On the basis of the encouraging results from various in vitro studies, the most active compounds were selected for further in vivo studies in animal models and preclinical development.

Introduction

Comprised of α and β subunits, integrins are heterodimeric proteins important for cell−cell and cell−extracellular matrix interactions.[1,2] Integrins serve as a transmembrane linker between their extracellular ligands and the cytoskeleton and modulate various signaling pathways. This means that they have the capacity to influence cell migration, differentiation, and survival during embryogenesis, angiogenesis, wound healing, immune and nonimmune defense mechanisms, hemostasis, and oncogenic transformation.[1] Many integrins are associated with pathological conditions.

The fibronectin receptor α5β1 integrin plays a key role during development of the vascular system, as confirmed in gene knock-out studies, gene expression analysis, and functional studies with integrin inhibitors.[3−5] Significant up-regulation of α5β1 on activated vascular endothelium was observed during angiogenesis, in tumor blood vessels, and after stimulation with angiogenic growth factors.[4−6] Inhibitory compounds would be of great interest as tools to unravel the role of α5β1 and possibly as therapeutic agents for pathological angiogenic conditions.

Many approaches for the design of novel ligands are based on the structure of the target protein and/or known ligands. Unfortunately, no unambiguous structural information on the binding conformation of α5β1 ligands is available. However, in the crystallographic structure of the related integrin αvβ3 in a complex with a cyclic pentapeptide (pdb ID 1L5G) also containing an arginine-glycine-aspartate motif (RGD), the Cβ distance between the Arg and the Asp is almost 9 Å, leading to an extended conformation of the RGD motif and a stretched arrangement of the charged side chains.[7]

A high degree of sequence identity is observed between α5β1 and αvβ3 (head groups α5/αv, 46%; β1/β3, 45%) and there is considerable sequence similarity between both integrins for the residues in proximity to the bound ligand in the αvβ3−peptide complex structure.[8] Besides, both integrins share a number of RGD-containing ligands. Therefore, in agreement with investigations of Marinelli et al.,[8] we assumed a binding mode similar to the one observed in αvβ3. On the basis of this assumption and published αvβ3 antagonists,[9] we designed new compounds that are able to competitively inhibit α5β1 binding to fibronectin. Here, we describe the synthesis, SAR, and biochemical characterization of a new class of α5β1 antagonists.

Chemistry

Compounds were selected from a virtual combinatorial library designed to cover the chemical space specific for RGD-derived compounds. Each virtual compound possesses a terminal basic 2-amino pyridine group with a linker of varying lengths, a terminal carboxylic acid with a linker of varying lengths, and a hydrophobic Cbz[a] group (Figure 1a). These three fragments were interconnected by trifunctional core fragments. Furthermore, the library design was directed by medicinal chemistry requirements to ensure synthetic accessibility.

3D conformations of the virtual compounds were generated and aligned to a template (for details, see Experimental Section). This template was derived from the X-ray structure of cyclo-[Arg-Gly-Asp-D-Phe-NMe-Val] bound to the receptor integrin αvβ3.[7] The template comprised the extended portion connecting the guanidino group of Arg and the carboxylic moiety of the Asp. This part of the ligand mediates 90% of the surface contacts to αvβ3 in the complex.

The alignments were scored with respect to their overall shape similarity to the template in combination with the overlap of the pharmacophoric features. SAR data for integrin ligands revealed positive effects of sulfonamides,[9] which were therefore included as building blocks in the virtual synthesis. This procedure identified a number of active compounds with IC_{50} values in a competitive integrin binding assay in the lower nanomolar range, among them compound **1** with an IC_{50} value of 3.7 nM.

For the optimization of **1**, we explored the influence of the Cbz group (R_1), the 2-amino pyridine substitution (R_2), and the hydrophobic mesitylene (R_3) on target activity and selectivity. In order to assess the chemical space around these three moieties,

* Corresponding author. Phone: +49-30-9 78 93-334. Fax: +49-30-9 78 93-105. E-mail: stragies@jerini.com.

[a] Abbreviations: ACN, acetonitrile; BSA, bovine serum albumin; Cbz, carboxybenzoyl; DCE, dichloroethane; DCM, dichloromethane; DIPEA, diisopropylethylamine; DMF, *N*,*N*-dimethylformamide; DMSO, dimethyl sulfoxide; ELISA, enzyme-linked immunosorbent assay; Fc, fragment of constant region of human immunoglobulin G1; HBTU, *O*-benzotriazole-*N*,*N*,*N*′,N′-tetramethyluronium hexafluorophosphate; HRP, horseradish peroxidase; IC_{50}, inhibition constant for 50% inhibition; MTBE, methyl *tert*-butyl ether; PIFA, phenyliodine(III) bis(trifluoracetate) also named [bis(trifluoroacetoxy)iodo]benzene; TFA, trifluoroacetic acid; THF, tetrahydrofuran; TMB, 3,3,5,5′-tetramethylethylenediamine; Tris, tris(hydroxymethyl)aminomethane.

10.1021/jm070002v CCC: $37.00
Published on Web 07/06/2007

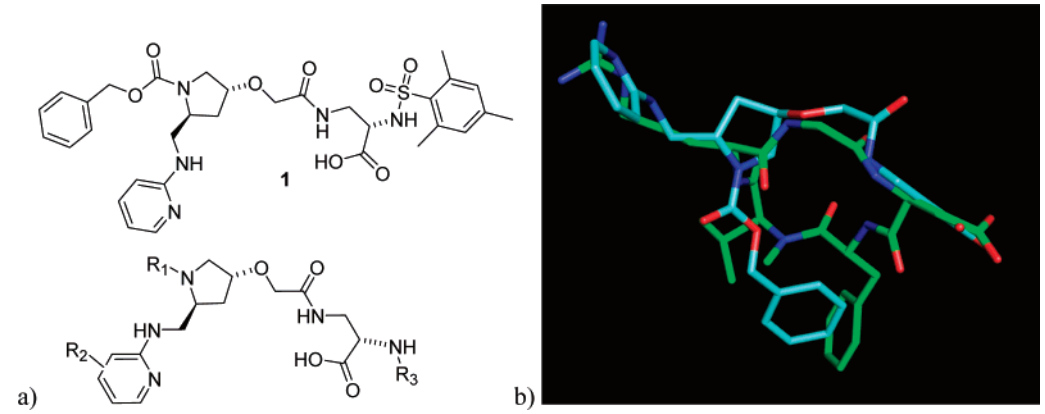

Figure 1. (a) Compound **1** and its generic structure with groups R_{1-3} (b) Compound **1** (cyan) superimposed on the X-ray structure of cyclo-[Arg-Gly-Asp-D-Phe-NMe-Val] from the complex with αvβ3 (green). For clarity, the sulfonamide moiety is not shown.

Scheme 1. Synthesis of R_1 Derivatives **1**, **7a**−**d**[a]

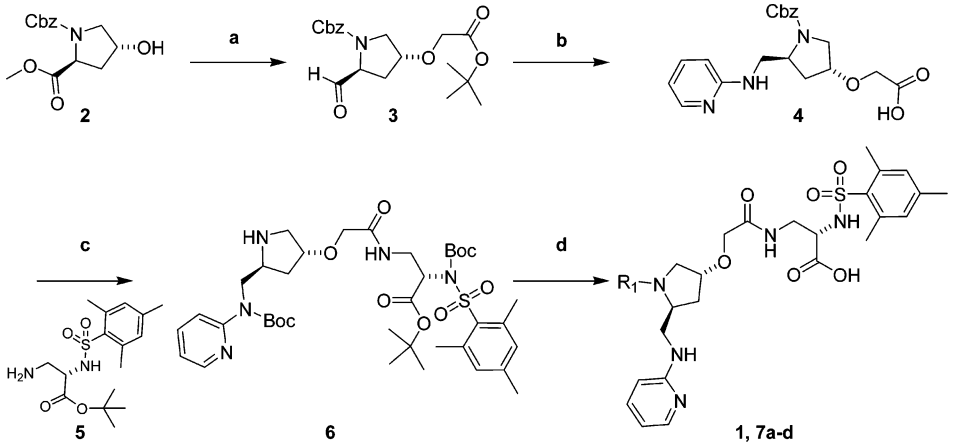

[a] Reagents and conditions: (a) (i) NaH, bromoacetic acid *tert*-butyl ester, THF; (ii) LiCl, $NaBH_4$, MeOH; (iii) SO_3−pyridine complex, DCM/DMSO; (b) (i) 2-aminopyridine, $Ti(OiPr)_4$, $NaHB(OAc)_3$, DCE; (ii) LiOH; (c) (i) HBTU, DIPEA, DMF; (ii) $(Boc)_2O$; (iii) H_2 Pd/C d) (i) R_1-Cl or R_1-Br, DIPEA, DCM; (ii) TFA.

different strategies were applied to introduce a diverse set of functional groups. Scheme 1 outlines the synthesis of derivatives with different R_1 moieties.

The synthesis of compounds **1** and **7a**−**d** started from Cbz-4-hyroxyproline methyl ester **2** (Scheme 1), which was first treated with NaH in THF and 3 equiv of bromoacetic acid *tert*-butyl ester to give the corresponding ether in 65% yield. The methyl ester was selectively reduced with $NaBH_4$ in the presence of LiCl in an ethanol/THF mixture and the obtained alcohols were directly oxidized with SO_3−pyridine complex in DCM/DMSO to give the aldehyde **3** in about 85% yield (two steps). The reductive amination with $Ti(OiPr)_4$ and $NaBH(OAc)_3$ in dichloroethane (DCE) gave the products as mixtures of *tert*-butyl ester and the corresponding isopropyl ester. Other conditions such as $NaCNBH_3$ in methanol did not lead to the desired product. Both esters were hydrolyzed with 3 equiv of LiOH to give compound **4** in about 55% yield. The coupling reaction with diamino propionic acid derivative **5** was performed with HBTU in DMF. Boc protection was achieved with $(Boc)_2O$ and DMAP in THF to yield 48% product. Under these conditions, the NH at the sulfonamide was also Boc-protected. After hydrogenation with Pd/C in isopropyl alcohol the precursor **6** was reacted with a variety of reagents such as isocyanates, alkyl bromides, and carboxylic acid chlorides. The final cleavage step proceeded quantitatively with TFA. The compounds **1** and **7a**−**d** were purified by HPLC (ACN/H_2O) and lyophilized.

Aldehyde **11** was prepared to incorporate other basic groups at the 2-aminopyridine position (R_2) (Scheme 2). The alcohol **8** was synthesized from Cbz-4-hydroxyproline methyl ester **2** according to Scheme 1. After protection of the OH-moiety as the *tert*-butylsilyl ether (TBDMS), the *tert*-butyl ester was hydrolyzed with LiOH to give **9** quantitatively. HBTU coupling and subsequent cleavage of the silyl ether with TBAF gave the alcohol **10** in 40% yield (two steps). Oxidation was performed with SO_3−pyridine to give aldehyde **11** in 91% yield. The reductive aminations were performed with $Ti(OiPr)_4$ and $NaBH(OAc)_3$ in DCE with different 2-aminopyridines. The compounds **12a**−**c** were obtained by TFA cleavage and purified by HPLC.

In the last sequence, the synthesis as described in Scheme 1 was modified. Starting from H-Hyp-OMe **13**, the different moieties were introduced at the NH using carboxylic acid chlorides in $NaHCO_3$/DCM (Scheme 3). Following the same sequence of alkylation, reduction, and oxidation, the aldehydes **3** and **15** were obtained in about 60% yields. Reductive amination and ester hydrolysis under the conditions mentioned above gave compounds **4** and **16a**−**c** in 41−63% overall yields. To explore the influence of different R_3 moieties, the diamino propionic acid derivatives **5**, **17**, and **18** were applied in the HBTU coupling reaction. In the final step, the *tert*-butyl esters were cleaved with TFA and the compounds **19c**−**k** were purified by HPLC.

The diamino propionic acid derivative **5** was prepared from L-asparagine **20** following the published procedure (Scheme 4).[9] Due to low yields in the coupling step of the unprotected L-asparagine with the corresponding carboxylic acids, the synthesis of amides **17** and **18** was modified. After the coupling

Scheme 2. Synthesis of 2-Aminopyridine (R_2) Derivatives **12a-c**[a]

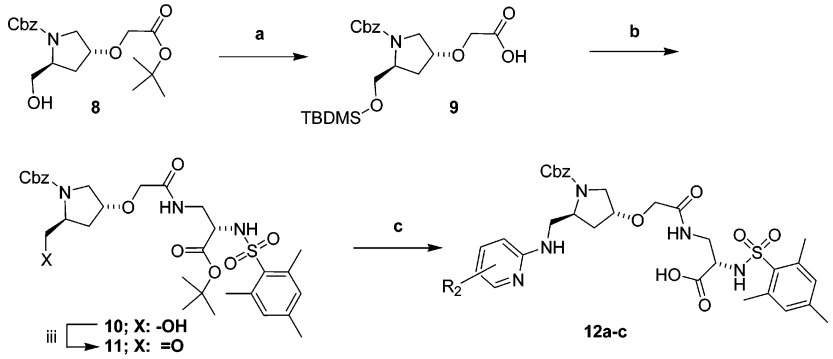

[a] Reagents and conditions: (a) (i) TBDMS−Cl, imidazole, DMF; (ii) LiOH; (b) (i) **5**, HBTU, DIPEA, DMF; (ii) TBAF; (iii) SO_3−pyridine complex, DCM/DMSO; (c) (i) 2-aminopyridines, $Ti(OiPr)_4$, $NaHB(OAc)_3$, DCE; (ii) TFA.

Scheme 3. Synthesis of Compounds **19a**−**k**[a]

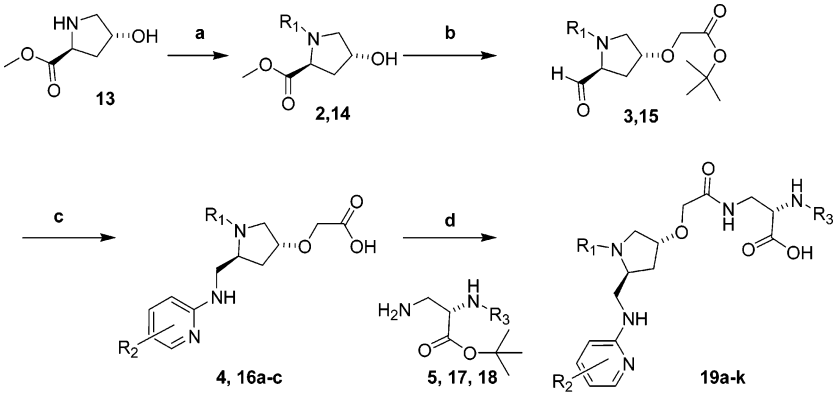

[a] Reagents and conditions: (a) (i) R_1−Cl, $NaHCO_3$, DCM; (b) (i) NaH, bromoacetic acid *tert*-butyl ester, THF; (ii) LiCl, $NaBH_4$, MeOH; (iii) SO_3−pyridine complex, DCM/DMSO; (c) (i) 2-aminopyridines, $Ti(OiPr)_4$, $NaHB(OAc)_3$, DCE; (ii) LiOH; (d) (i) HBTU, DIPEA, DMF; (ii) TFA.

Scheme 4. Synthesis of the Diaminopropionic Acid Derivatives **5**, **17**, and **18**[a]

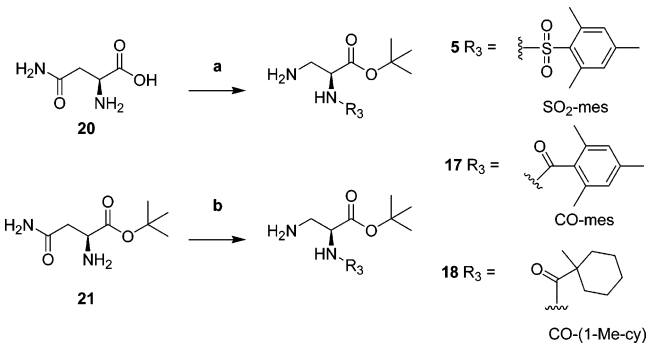

[a] Reagents and conditions: (a) (i) Cl−SO_2−aryl, THF/H_2O, NEt_3; (ii) NaOH, Br_2, H_2O; (iii) isobutene, H_2SO_4, dioxane; (b) (i) aryl or alkyl carboxylic acid, HBTU, DIPEA, DMF; (ii) phenyliodine(III) bis(trifluoracetate) (PIFA), pyridine, ACN.

step with asparagine *tert*-butyl ester the Hofmann rearrangement of the terminal amide into an amine was achieved by utilizing phenyliodine(III) bis(trifluoracetate) (PIFA) in the presence of pyridine in ACN.[10] The diamino propionic acid derivatives **17** and **18** were obtained in an overall yield of 66% and 67%, respectively.

Results and Discussion

Approximately 200 derivatives of this scaffold class obtained from the described syntheses (Schemes 1−3) were analyzed to elucidate the influence of R_1, the aminopyridine R_2, and the hydrophobic part R_3 on integrin activity and selectivity. Although the activity of compound **1** was already in the nanomolar range, it was planned to increase its potency. In addition, selectivity especially toward integrins $\alpha v\beta 3$ and $\alpha v\beta 5$ had to be improved. Activities were monitored in ELISAs with the corresponding integrins: the activities of selected compounds toward integrins $\alpha 5\beta 1$ and $\alpha v\beta 3$ are shown in Table 1.

Table 1. IC_{50} Values for Inhibitors of Integrin $\alpha 5\beta 1$ and $\alpha v\beta 3$ in a Competitive Integrin Binding Assay

Compound	Structure (R_2 = H, R_3 = SO_2-mes) R_1	IC_{50} (nM) $\alpha 5\beta 1$	$\alpha v\beta 3$
1	Cbz	3.7	16
7a		15	9
7b		6	36
7c	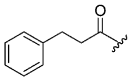	25	38
7d	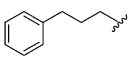	670	nd.
7e	H	286	nd.

Compounds **7a**−**e** have different R_1 moieties and illustrate the influence of the phenyl ring and the carbamate moiety of the Cbz group of compound **1**. The comparable activities of **7a** and **7b** demonstrate that inhibition similar to that of the Cbz

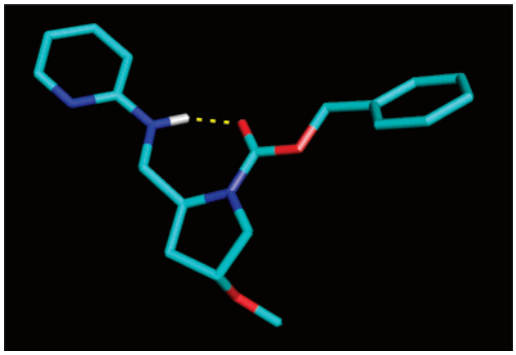

Figure 2. Pyrrolidine partial structure of compound **1** stabilized by a hydrogen bond.

Table 2. IC_{50} Values for Inhibitors of Integrin α5β1 and αvβ3 in a Competitive Integrin Binding Assay

		IC_{50} (nM)	
compd	structure[a] R_2	α5β1	αvβ3
12a	4-OMe	1.1	2.4
12b	4-Cl	445	nd.
12c	6-Me	231	21

[a] R_1 = Cbz, R_3 = SO_2-mes.

group could be achieved with other hydrophobic moieties and that the carbamate could be replaced by amides. This was confirmed with derivative **7c**. In contrast, the carbonyl group is essential, as underlined by the dramatic decrease in activity of **7d** and **7e**.

NMR measurements for compound **1** indicate a hydrogen bond between the amino group of the 2-aminopyridine and the carbonyl group in R_1, pointing to a 7-membered ring structure (Figure 2). If such a hydrogen bond is formed in the receptor-bound conformation as well, the loss of entropy upon binding due to freezing of rotatable bonds is reduced compared to a molecule without a hydrogen bond in this position. The reduced loss of entropy leads to more negative free binding energy and thus to very high activities, whereas significantly lower activities are observed for molecules with unrestricted conformational flexibility that are unable to form an intramolecular hydrogen bond (e.g., compound **7d**).[11]

It was found that a variety of aromatic and alkyl amides and carbamates were tolerated in this position. This diverse set of highly active compounds was narrowed down by determining ADME properties and ranking the compounds accordingly. For example, stability in human microsomes was measured at compound concentrations of 1 μM. After reviewing the obtained results, it was found that lead compound **1** showed only moderate stability of 43% after 1 h. This property could be significantly improved by replacing the Cbz group by the 3,3-dimethylbutyric acid amide function. The microsomal stability of **7b** was 70% and represented the favored replacement of the Cbz moiety of compound **1**.

In parallel, the effects of different substituents at the pyridine ring R_2 were investigated. A clear SAR of the pyridine ring substituents was obtained. A correlation between the electron acceptance/donating nature, e.g., reflected by the Hammett σ constants, of the substituents in position 4 and the IC_{50} values (Table 2) was observed over the investigated range.

Activity decreases from compound **12a** with an electron-donating 4-methoxy moiety to compound **1** with a neutral 4-hydrogen atom and then derivative **12b** with an electron-accepting 4-chloro atom [1.1 nM (4-OMe) < 3.7 nM (4-H) < 445 nM (4-Cl)]. In addition to these findings, a loss in activity

Table 3. IC_{50} Values for Inhibitors of Integrin α5β1, αvβ3, αvβ5, αIIbβ3, and α3β1 in a Competitive Integrin Binding Assay

Compound	Structure			IC_{50} (nM)				
	R_1	R_2	R_3	α5β1	αvβ3	αvβ5	αIIbβ3	α3β1
1	Cbz	H	SO_2-mes	3.7	16	330	9000	>200000
19a	Cbz	H	SO_2-Ph	86	6.3	260	12000	nd.
19b	Cbz	H	CO-Ph	155	140	nd.	nd.	nd.
19c	Cbz	H	CO-mes	3.5	~30000	~30000	>50000	~36000
19d	Cbz	H	CO-(1-Me-cy)	1.7	880	550	>50000	nd.
19e		H	CO-mes	1.6	16000	>50000	>50000	nd.
7b		H	SO_2-mes	6	36	245	8000	nd.
12a	Cbz	4-OMe	SO_2-mes	1	2.4	19	7.700	nd.
19f		H	CO-(1-Me-cy)	1.4	1600	2300	>50000	nd.
19g	Cbz	4-OMe	CO-mes	0.54	~3400	2700	~50000	~20000
19h		4-OMe	SO_2-mes	0.9	4	29	11000	n.d.
19i		4-OMe	CO-mes	0.55	3300	6800	>50000	~13000
19j	Cbz	4-OMe	CO-(1-Me-cy)	0.8	690	3100	>50000	~30000
19k		4-OMe	CO-(1-Me-cy)	0.55	980	4300	>50000	~50000

of almost 2 orders of magnitude was observed with the 6-methyl derivative **12c** compared to the 6-H derivative **1**. This significant drop in activity cannot be explained by the electronic nature of a methyl moiety. Therefore, this effect was attributed to steric restriction at this position.

In summary, for lead compound **1**, 3,3-dimethylbutyric acid amide was identified as a suitable replacement for the Cbz group, inducing sufficient activity on the target and conferring high microsomal stability. Introduction of a methoxy moiety in position 4 of the aminopyridine moiety led to improved potency.

Control of Integrin Selectivity. All improvements at this stage resulted in potent α5β1/αvβ3 dual specific inhibitors. In all cases, the measured integrin α5β1 activities were on the same order of magnitude as for integrin αvβ3. To improve selectivity toward other integrins, the properties of the hydrophobic side chain R_3 were explored. In addition to their activity on integrin αvβ3, the inhibitory potential on other related integrins such as αvβ5, αIIbβ3, and α3β1 were monitored (Table 3).

Compound **1** showed no relevant interaction with the platelet aggregation receptor αIIbβ3 and another β1 integrin (α3β1). Besides the nanomolar inhibition of integrin αvβ3, moderate interaction with integrin αvβ5 was observed.

The influence of methyl groups at the mesitylene group and the role of the sulfonamide were explored with derivatives **19a** and **19b** (prepared in analogy to Scheme 3). The significant drop in activity of the phenyl sulfonamide **19a** demonstrates the impact of the two 2,6-methyl groups. However, compared to the sulfonamide **19a**, only a slight decrease in activity of the corresponding benzamide **19b** was seen. Also, neither derivative influenced the low selectivity toward integrin αvβ3.

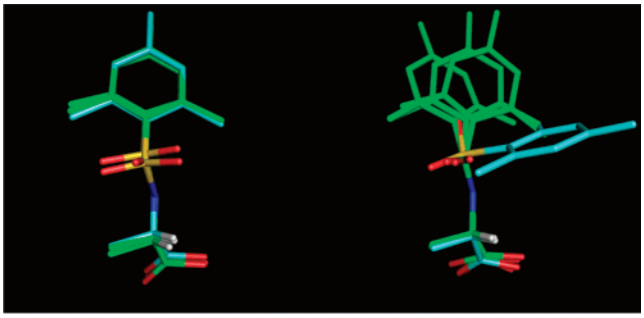

Figure 3. Left: Shared conformational space for amide (green) and sulfonamide (cyan) in R_3. The minimum amide structure can be imitated by a sulfonamide. Right: The sulfonamide (cyan) can adopt a minimum structure that cannot be adopted by the amide.

Surprisingly, the corresponding mesitylene amide **19c** has an IC_{50} similar to the sulfonamide **1** of 3.5 nM. Moreover, compound **19c** revealed a remarkable selectivity profile with a 10 000−15 000-fold selectivity to all other integrins shown in Table 3. This finding was considered to be an important breakthrough during the development of potent and selective integrin $\alpha5\beta1$ inhibitors. Further investigations showed that particularly the 2,6-substitution pattern at the aromate guaranteed selectivity. In addition, it was found that this property of the mesitylene amide moiety was not a unique feature for this scaffold class: replacement of sulfonamide groups by a mesitylene amide in other integrin $\alpha v\beta3$ binding scaffolds known from the literature or found by our group also improved selectivity in favor of integrin $\alpha5\beta1$ in all cases.

The reason for the high specificity of compounds containing an amide in R_3 compared to the sulfonamides is most likely due to the difference in conformational flexibility and therefore the coverage of the conformational space by this residue. Analysis of the conformational space covered by the amide/sulfonamide showed that the mesitylene group in the sulfonamide can match all orientations of this group accessible to the corresponding amide. In contrast, the amide cannot access the orientations of the mesitylene moiety found in the sulfonamide (Figure 3). Ab initio calculations have shown that the rotational barrier of amide bonds is twice as high as the rotational barrier of sulfonamide bonds.[12] Therefore, a possible explanation for the obtained selectivity is that the integrin $\alpha5\beta1$ binding pocket can accommodate both types of ligands, the sulfonamide and the amide, demanding the conformation shared by both molecules. Binding to $\alpha v\beta3$ demands another conformation, which can only be adopted by the more flexible sulfonamide.

Reasonable selectivity could also be reached with bulky alkyl substituents replacing the mesitylene. An increase in selectivity by a factor of 520 was observed by replacing the sulfonamide in **1** by a 1-methylcyclohexyl amide (**19d**). It is worth noting that the diastereomer with an opposite configuration at the diaminopropionic acid only shows a 2-fold decrease in activity.

Compared with the Cbz derivatives **19c** and **19d**, the potency of the 3,3-dimethylbutyric acid amides **19e** and **19f** remained unchanged, which was not seen with derivative **7b**. Nevertheless, a slight increase in selectivity was observed. These results were in contrast to our previous findings where we observed no impact on selectivity by this group.

An increase of activity by a factor of 4−6 was achieved by introducing 4-methoxy-2-aminopyridine as a basic group (compounds **12a**, **19g**−**k**). 4-Methoxy-2-aminopyridine compounds expressed a similar selectivity toward other integrins, as reported for the unsubstituted aminopyridine series. Additive effects to the activity on integrin $\alpha5\beta1$ were seen for 4-methoxy substitution of the 2-aminopyridine, the mesitylene amide/1-methylcyclohexyl amide and the 3,3-dimethylbutyric acid amide.

The high activity of compound **19i** was also confirmed in a cell adhesion assay. The assay was performed on fibronectin with HEK293 cells intrinsically expressing integrin $\alpha5\beta1$. Thus, this type of assay is a more advanced functional assay, since it tests the inhibitory activity on integrin $\alpha5\beta1$ presented on the cell surface. An IC_{50} of 50 nM in this cell assay reflects the high activity of the compound in the protein binding assay. Additionally, the inhibitory activity was further confirmed in other in vitro assays, such as integrin-mediated phosphorylation, migration, and cell survival (data not shown).

On the basis of these encouraging results, the most active compounds were selected for in vivo studies. These compounds showed inhibitory activity in several pharmacological models with pathological angiogenesis. Such models included several species such as monkey, rabbit, and mouse. The in vivo activities of these integrin $\alpha5\beta1$ inhibitors were proven in ocular and tumor angiogenesis models after systemic and local administration.[5,13−15]

Conclusions

The synthesis of a new class of highly active and selective integrin $\alpha5\beta1$ antagonists is reported. Different synthesis strategies were applied to assess the chemical space around the essential pharmacophore groups. Starting structures were identified using information available on the structure of a similar integrin ($\alpha v\beta3$) complexed to a peptidic ligand and the SAR of available nonpeptidic ligands for this and other integrins. The switch from a sulfonamide moiety to a mesitylene amide moiety represents a general feature for achieving selectivity toward other related integrin receptors by decreasing the amount of local conformational freedom.

Selected compounds were evaluated in a number of assays. The promising in vitro and in vivo activities confirmed the proposed mode of action for selective integrin $\alpha5\beta1$ antagonists in relevant animal models with pathological angiogenesis and tumor growth.[5,13−15] The most active compound will be further evaluated in clinical development for ocular angiogenesis in age-related macular degeneration.

Experimental Section

The reagents used were purchased from Sigma-Aldrich-Fluka (Deisenhofen, Germany), Bachem (Heidelberg, Germany), Lancaster (Mühlheim/Main, Germany), Merck Eurolab (Darmstadt, Germany), Merck Biosciences, Darmstadt, Germany), and Acros (Geel, Belgium, distributor Fisher Scientific GmbH, Schwerte, Germany) and used at the specified quality without further purification. For analytical TLC, Merck silica gel 60 F254 plates were used, and column chromatography was performed on Merck silica gel 60 (0.015−0.040 mm). All products were analyzed by HPLC−MS on a Surveyor HPLC combined with an LCQ classic or Advantage (all Thermo Electron) equipped with an ESI-source. ^{1}H NMR spectra were measured in $CDCl_3$ or DMSO-d_6 with a Varian 300 and 500 MHz spectrometer; chemical shifts are expressed in ppm relative to TMS as internal standard and coupling constants (J) are in Hz.

Virtual Synthesis and Flexible Alignment. The rigid template was the RGD tripeptide of the peptidic ligand in the complex structure 1L5G. A virtual library of the general scheme base−C_nH_{2n}−core−C_nH_{2n}−acid where $n = 0, 1, 2, 3$ was generated using trifunctional building blocks from the Available Chemicals Directory (ACD, MDL Information Systems, San Ramon, CA). The virtual compounds were flexibly aligned on the rigid template using the approach of Labute et al.[16] implemented in the MOE package (2003.02) of the Chemical Computing Group (Montreal, Canada). Scoring the pharmacophore overlap used pseudoenergy, which

includes the average strain energy and the alignment score for the aligned molecule. To achieve good alignment of the acidic and basic terminal groups, the weight for the similarity terms "charge" and "acid_base" was set to 5, the weights for "donor", "acceptor", "volume", and "hydrophobe" were 1, and that for "aromatic" was 2.

Conformational Analysis. Conformational analysis was performed using the MOE package of Chemical Computing Group[16] and the Merck force field (MMFF94).[17] For the sulfonamide and the amide, systematic rotations around the amide/sulfonamide bond and the mesitylene moiety were performed in 10° steps. All conformations were relaxed by keeping both bonds fixed. The resulting conformations were filtered (energy cutoff 10 kcal/mol) and clustered (rmsd value for mesitylen moiety less than 0.5 Å).

General Procedure A for the Synthesis of Compounds 1, 7a−d. Synthesis of 2*S*,4*R*-4-*tert*-Butoxycarbonylmethoxypyrrolidine-1,2-dicarboxylic Acid 1-Benzyl Ester 2-Methyl Ester. NaH (6.70 g, 166 mmol, 60% in paraffin), 61.4 mL (416 mmol) of *tert*-butyl bromoacetate, and 4.1 g (11 mmol) n-$Bu_4N^+I^-$ were suspended under argon in 400 mL of absolute THF. Cbz-Hyp-OMe (**2**) (38.7 g, 111 mmol), dissolved in 100 mL of absolute THF, was added slowly to the reaction mixture and stirred overnight. After addition of 20 mL of saturated NH_4Cl solution and 300 mL of water, the reaction mixture was extracted three times with 500 mL of MTBE. The combined organic layers were dried with Na_2SO_4, and the solvent was removed by an evaporator. The crude reaction mixture was dissolved in 200 mL of MeOH and the paraffin oil was removed. After evaporation of the solvent, the crude product was purified by chromatography on silica gel using ethyl acetate/hexane. Yield: 35.4 g (65%). ^{1}H NMR (DMSO-d_6): δ = 7.42−7.24 (m, 5H), 5.09 (s, 2H), 4.96 (d, 1H, J = 9.6), 4.31 (dt, 1H, J = 16.1, J = 7.8), 4.18 (m, 1H), 3.65 (s, 2H), 3.54 (s, 3H), 3.54 (dt, 1H, J = 4.4, J = 11.7), 2.37 (m, 1H), 2.00 (m, 1H), 1.42 (s, 9H). ^{13}C NMR (DMSO-d_6) (partial signal doubling due to Cbz rotameres): δ = 172.6 (C_q), 172.3 (C_q), 169.4 (C_q), 154.1 (C_q), 153.5 (C_q), 136.7 (C_q),136.5 (C_q), 128.5 (CH), 128.4 (CH), 128.3 (CH), 127.9 (CH), 127.8 (CH), 127.5 (CH), 127.3 (CH), 80.8 (C_q), 77.63 (CH_2), 76.8 (CH_2), 69.2 (CH), 66.2 (CH_2), 66.2 (CH_2), 57.7 (CH_2), 57.3 (CH_2), 52.2 (CH_2), 52.0 (CH_2), 51.8 (CH), 35.8 (CH_2), 34.9 (CH_2), 27.7 (CH_3). LCMS: m/z 394.5 [MH^+].

Synthesis of 2*S*,4*R*-4-*tert*-Butoxycarbonylmethoxy-2-hydroxymethylpyrrolidine-1-carboxylic Acid Benzyl Ester (8). 2*S*,4*R*-4-*tert*-Butoxycarbonylmethoxy-pyrrolidine-1,2-dicarboxylic acid 1-benzyl ester 2-methyl ester (35 g, 90 mmol), 7.6 g (180 mmol) of LiCl, and 6.8 g (180 mmol) of $NaBH_4$ were dissolved in 590 mL of absolute THF and 295 mL of absolute EtOH at 0 °C. The reaction mixture was stirred overnight and the temperature was kept between 0 and 10 °C. Then 150 mL of 2 M HCl and 50 mL of saturated $NaHCO_3$ were added to the solution. The reaction mixture was concentrated, the aqueous layer was extracted twice with 600 and 300 mL of ethyl acetate, and the combined organic layers were washed with saturated $NaHCO_3$ and NaCl solution. The organic layer was dried over Na_2SO_4 and the solvent was removed by an evaporator. The product was crystallized from toluene (5% DCM) and hexane at 0 °C. Yield: 27.8 g (85%). ^{1}H NMR (DMSO-d_6): δ = 7.40−7.28 (m, 5H), 5.05 (s, 2H), 4.73 (m, 1H), 4.13 (m, 1H), 3.97 (s, 2H), 3.84 (m, 1H), 3.60−3.29 (m, 4H), 2.00 (m, 2H), 1.41 (s, 9H). ^{13}C NMR (DMSO-d_6) (partial signal doubling due to Cbz rotameres): δ = 169.4 (C_q), 154.2 (C_q), 137.0 (C_q), 128.3 (CH), 127.7 (CH), 127.5 (CH), 127.4 (CH), 127.4 (CH), 80.7 (C_q), 77.6 (CH_2), 77.0 (CH_2), 67.4 (CH), 66.2 (CH_2), 65.9 (CH_2), 65.7 (CH_2), 61.2 (CH_2), 59.7 (CH), 57.8 (CH_2), 57.2 (CH_2), 52.4(CH_2), 52.0 (CH_2), 27.7 (CH_3). LCMS: m/z 366.4 [MH^+].

Synthesis of 2*S*,4*R*-4-Carboxymethoxy-2-(pyridin-2-ylaminomethyl)pyrrolidine-1-carboxylic Acid Benzyl Ester (4). 3 (5.0 g, 13.7 mmol) and 28.6 mL (206 mmol) of NEt_3 were dissolved in 280 mL of DCM/DMSO (v/v = 3/1) and cooled to 0 °C. SO_3−pyridine complex (26.17 g, 164 mmol) was added and the reaction mixture was stirred for 2 h. DCM was removed by an evaporator and the crude reaction mixture was poured into 500 mL of ethyl acetate and extracted with H_2O, saturated $NaHCO_3$, and NaCl solution. The organic layer was dried over Na_2SO_4 and the solvent was removed by an evaporator.

The crude reaction mixture was dissolved in 500 mL of dichloroethane, and 2.58 g (27.4 mmol) of 2-aminopyridine and 10.2 mL (34.3 mmol) of $Ti(OiPr)_4$ were added. After stirring overnight at 60 °C, 29.4 g (139 mmol) of $NaBH(OAc)_3$ was added at room temperature and the reaction was stirred for additional 4 h. The solvent was removed by an evaporator and the reaction mixture was dissolved in 500 mL of ethyl acetate and extracted with 0.1 M HCl, saturated $NaHCO_3$, and NaCl solution. The reaction mixture was dried with Na_2SO_4 and the solvent was removed by an evaporator.

The crude reaction mixture was dissolved in 300 mL of THF/H_2O (v/v = 2/1), 1.0 g (41.8 mmol) of LiOH was added, and the solution was stirred for 4 h. THF was evaporated and the solution was acidified with 3 M HCl to pH ≈ 4. The solution was extracted three times with 100 mL of DCM and dried with Na_2SO_4 and the solvent was removed by an evaporator. The product was crystallized from THF as the HCl salt. Yield: 3.1 g (55%). ^{1}H NMR (DMSO-d_6): δ = 8.87 (s, broad, 1H), 8.01−7.82 (m, 2H), 7.34 (m, 5H), 7.17 (t, 1H, J = 8.8), 7.02−6.78 (m, 2H), 5.07 (m_c, 2H), 4.23−4.08 (m, 2H), 4.02 (s, 2H), 3.74−3.34 (m, 4H), 2.20 (m_c, 1H), 1.92 (m_c, 1H). ^{13}C NMR (DMSO-d_6) (partial signal doubling due to Cbz rotameres): δ = 171.5 (C_q), 171.3 (C_q), 154.9 (C_q), 154.5 (C_q), 153.1 (C_q), 152.9 (C_q), 136.7 (C_q), 136.5 (C_q), 128.7 (CH), 128.6 (CH), 128.3 (CH), 128.2 (CH), 127.7 (CH), 127.6 (CH), 127.3 (CH), 112.6 (CH), 111.9 (CH), 85.9 (CH), 77.2 (CH), 77.0 (CH), 66.0 (CH_2), 65.5 (CH_2), 55.0 (CH), 54.4 (CH), 51.8 (CH_2), 49.8 (CH_2), 46.2 (CH_2), 44.0 (CH_2). 34.2 (CH_2), 33.9 (CH_2). LCMS: m/z 386.3 [MH^+].

Synthesis of 2*S*,3*R*,5*S*-4-(2-{[2-*tert*-Butoxycarbonyl-2-(2,4,6-trimethylbenzenesulfonyl-*tert*-butoxycarbonylamino)-2-(*tert*-butoxycarbonyl)ethyl]amino}-2-oxoethoxy)-2-[(*tert*-butoxycarbonylpyridin-2-ylamino)methyl]pyrrolidine-1-carboxylic Acid Benzyl Ester. 4 (3.0 g, 7.1 mmol), 2.7 g (7.8 mmol) of 3*S*-3-amino-2-(2,4,6-trimethylbenzenesulfonylamino)propionic acid *tert*-butyl ester (**5**), 3.26 g (7.8 mmol) of HBTU, and 4.5 mL (31.2 mmol) of DIPEA were dissolved in 50 mL of DMF and stirred for 2.5 h. The solvent was removed by an evaporator and the crude product was dissolved in 600 mL of ethyl acetate. The organic layer was extracted with saturated $NaHCO_3$ and NaCl solution and dried with Na_2SO_4, and the solvent was removed by an evaporator. The crude reaction mixture was dissolved in 100 mL of absolute THF. $(Boc)_2O$ (2.77 g, 59.4 mmol) and DMAP were added. After 3 days at room temperature an additional 0.92 g (4.2 mmol) of $(Boc)_2O$ and after 1 day an additional 1.84 g (8.5 mmol) of $(Boc)_2O$ were added and the mixture stirred for 24 h. The solvent was removed by an evaporator and the crude product was dissolved in 500 mL of ethyl acetate. The organic layer was extracted with saturated $NaHCO_3$ and NaCl solution and dried with Na_2SO_4, and the solvent was removed by an evaporator. The crude product was purified by chromatography on silica gel using ethyl acetate/hexane. Yield: 3.11 g (48%). ^{1}H NMR (DMSO-d_6): δ = 8.27 (dd, 1H, J = 3.4, 13.2), 7.75−7.61 (m, 2H), 7.44 (t, 1H, J = 5.8), 7.07 (m, 3H), 5.03 (dd, 1H, J = 5.3, 7.8), 4.99−4.82 (m, 2H), 4.18 (m, 2H), 4.08 (m, 2H), 3.82 (s, 2H), 3.75 (m, 2H), 3.51 (dd, 1H, J = 12.2, J = 12.9), 3.21 (dd, 1H, J = 4.4, 11.2), 2.54 (s, 6H), 2.06 (m, 2H), 1.92 (m, 2H), 1.39 (s, 21H), 1.28(s, 9H). ^{13}C NMR (DMSO-d_6): δ = 169.2 (C_q), 166.6 (C_q), 162.2 (C_q), 153.5 (C_q), 150.2 (C_q), 147.2 (CH), 143.1 (CH), 140.0 (CH), 131.7 (CH), 128.2 (CH), 127.6 (CH), 127.4 (CH), 127.3 (CH), 84.3 (C_q), 82.16 (C_q), 80.6 (C_q), 80.4 (C_q), 77.6 (CH_2), 73.5 (CH), 67.8 (CH_2), 66.0 (CH), 65.8 (CH), 57.8 (CH_2), 55.4 (CH), 35.7 (CH_2), 30.7 (CH_2), 27.7 (CH_3), 27.4 (CH_3), 27.3 (CH_3), 22.4 (CH_3), 20.5(CH_3). LCMS: m/z 910.6 [MH^+].

Synthesis of 2*S*,3*R*,5*S*-3-(2-{5-[(*tert*-Butoxycarbonylpyridin-2-ylamino)methyl]pyrrolidin-3-yloxy}acetylamino)-2-[*tert*-butoxycarbonyl(2,4,6-trimethyl-benzenesulfonyl)amino]propionic Acid *tert*-Butyl Ester (6). The compound obtained from the previous reaction (1.30 g, 1.42 mmol) was dissolved in 25 mL of isopropyl alcohol, and 130 mg of Pd (10% on carbon) was added. The reaction mixture was stirred under a H_2 atmosphere for 12 h

and filtered over Celite, and the solvent was removed by an evaporator. The crude product was purified by chromatography on silica gel using ethyl acetate/MeOH. Yield: 820 mg (74%). ^{1}H NMR (DMSO-d_6): δ = 8.27 (dd, 1H, J = 0.9, 4.9), 7.72−7.62 (m, 2H), 7.47 (d, 1H, J = 8.3), 7.07 (m, 3H), 5.02 (dd, 1H, J = 4.9, 8.3), 4.03 (m_c, 1H), 3.92−3.62 (m_c, 7H), 3.43 (t, 1H, J = 6.8), 2.80 (d, 2H, J = 2.9), 2.53 (s, 6H), 1.84 (dd, 1H, J = 7.3, J = 14.2), 1.40 (s, 21H), 1.28 (s, 9H). ^{13}C NMR (DMSO-d_6): δ = 169.6 (C_q), 166.7 (C_q), 154.3 (C_q), 153.5 (C_q), 150.2 (C_q), 147.3 (CH), 143.1 (C_q), 140.0 (C_q), 137.2 (CH), 133.6 (C_q), 131.7 (CH), 120.4 (CH), 119.9 (CH), 84.3 (C_q), 82.2 (C_q), 80.8 (CH), 80.3 (C_q), 67.5 (CH_2), 59.7 (CH_2), 57.9 (CH), 55.9 (CH), 51.3 (CH_2), 50.4 (CH_2), 35.9 (CH_2), 27.8 (CH_3), 27.5 (CH_3), 27.3 (CH_3), 22.4 (CH_3), 20.5 (CH_3). LCMS: *m/z* 778.6 [MH$^+$].

Synthesis of 2*S*,3*R*,5*S*-3-{2-[1-(3,3-Dimethylbutyryl)-5-(pyridin-2-ylaminomethyl)pyrrolidin-3-yloxy]acetylamino}-2-(2,4,6-trimethylbenzenesulfonylamino)propionic Acid (7b). 6 (15 mg, 0.02 mmol) and 300 μL of DIPEA were dissolved at 0 °C in 1 mL of DCM. 3,3-Dimethylbutyryl chloride (4 mg, 0.02 mmol), dissolved in 200 μL of DCM, was added, and the solution was stirred at 0 °C for 2 h. The solvent was evaporated and the crude reaction mixture was redissolved in 300 μL of TFA and stirred for 2 h at room temperature. After evaporation of the TFA, the product was purified by HPLC and freeze-dried using ACN/H_2O. Yield: 11.7 mg (83%, TFA salt). ^{1}H NMR (DMSO-d_6): (partial signal doubling due to rotameres) δ = 13.41 (s, broad, 1H), 8.62 (s, broad, 1H), 7.97 (d, 1H, J = 5.9), 7.95 (d, 1H, J = 8.8), 7.90 (m, 1H), 7.69 (t, 1H, J = 5.9), 7.10 (m, 1H), 6.97 (s, 2H), 6.85 (t, 1H, J = 6.6), 4.20 (m, 1H), 4.15 (m, 1H), 3.87−3.67 (m, 6H), 3.60 (dd, 1H, J = 5.1, J = 11.7), 3.55 (m, 1H), 3.43 (m, 2H), 3.17 (m, 1H), 2.52 (s, 3H), 2.50 (m, 6H), 2.17 (m, 1H), 1.96 (m, 1H), 0.98 (s, 9H). LCMS: *m/z* 618.8 [MH$^+$].

General Procedure B for the Synthesis of Compounds 12a−c. Synthesis of 2*S*,4*R*-2-(*tert*-Butyldimethylsilanyloxymethyl)-4-carboxymethoxypyrrolidine-1-carboxylic Acid Benzyl Ester (9). 8 (1.5 g, 4.1 mmol), 558 mg (8.2 mmol) of imidazole, and 800 mg (8.2 mmol) of *tert*-butyldimethylsilyl chloride were dissolved in 50 mL of DMF and stirred overnight. The reaction mixture was dissolved in 300 mL of MTBE; extracted with water, saturated $NaHCO_3$, and NaCl solution; and dried with Na_2SO_4. The solvent was removed by an evaporator. The crude reaction mixture was dissolved in 40 mL of MeOH, and 688 mg (16.4 mmol) of LiOH was added. After stirring overnight, NH_4Cl was added, and the solids were filtered off. The solvent was removed by an evaporator and the product was purified by chromatography on silica gel using ethyl acetate/hexane. Yield: 2.08 g (>116%, siloxane). ^{1}H NMR (DMSO-d_6): δ = 7.94 (m, 1H), 7.37 (m, 3H), 7.30 (m, 1H), 5.06 (m, 3H), 4.16 (m, 1H), 3.84 (m, 1H), 3.64−3.15 (m, 4H), 2.06 (m, 1H), 2.00 (m, 2H) 1.02 (s, 9H), 0.99 (s, 6H). ^{13}C NMR (DMSO-d_6): δ = 185.4 (C_q), 172.0 (C_q), 128.3 (CH), 127.7 (CH), 127.3 (CH), 76.7 (CH), 67.2 (CH_2), 65.8 (CH_2), 61.2 (CH_2), 57.8 (CH), 51.7 (CH_2), 22.1 (CH_3), 15.1 (C_q), −0.3 (CH_3). LCMS: *m/z* 367.4 [M-(*tert*-butyl)$^+$].

Synthesis of 2*S*,3*R*,5*S*-4-{[2-*tert*-Butoxycarbonyl-2-(2,4,6-trimethylbenzenesulfonylamino)ethylcarbamoyl]methoxy}-2-hydroxymethylpyrrolidine-1-carboxylic Acid Benzyl Ester (10). 9 (1.0 g, 2.3 mmol), 884 mg (2.33 mmol) of HBTU, and 795 μL (4.7 mmol) of DIPEA were dissolved in 20 mL of DMF and stirred for 10 min. **5** (800 mg, 2.33 mmol), dissolved in 5 mL of DMF, was added and the solution was stirred overnight. The solvent was removed by an evaporator and the crude product was dissolved in 400 mL of ethyl acetate. The organic layer was extracted with saturated $NaHCO_3$ and NaCl solution and dried with Na_2SO_4, and the solvent was removed by an evaporator. The crude product was dissolved in 50 mL of dry THF. TBAF (8.5 mL, 1 M in THF) was added and the solution was stirred for 2 h. An additional 6.5 mL of 1 M TBAF in THF was added and the solution was stirred overnight. The solvent was removed by an evaporator and the crude product was dissolved in 400 mL of ethyl acetate. The organic layer was extracted with water, saturated $NaHCO_3$, and NaCl solution and dried with Na_2SO_4, and the solvent was removed by an evaporator. The crude product was purified by chromatography on silica gel using ethyl acetate/hexane. Yield: 600 mg (40%). ^{1}H NMR (DMSO-d_6): δ = 8.06 (d, 1H, J = 8.8), 7.73 (t, 1H, J = 5.8), 7.35 (m, 5H), 6.98 (s, 2H), 5.05 (s, 2H), 4.75 (m, 1H), 4.09 (m, 1H), 3.84 (m, 1H), 3.76 (t, 2H, J = 15.2), 3.67−3.35 (m, 3H), 3.17 (m, 2H), 2.53 (s, 6H), 2.50 (t, 1H, J = 1.9), 2.22 (s, 3H), 2.04 (m, 2H), 1.56 (m, 2H), 1.13 (s, 9H). ^{13}C NMR (DMSO-d_6): δ = 169.1 (C_q), 168.8 (C_q), 154.1 (C_q), 141.4 (C_q), 138.4 (C_q), 136.9 (C_q), 134.4 (C_q), 131.4 (CH), 128.3 (CH), 127.7 (CH), 127.4 (CH), 80.7 (CH_2), 77.6 (CH), 67.6 (CH_2), 61.1 (CH_2), 57.9 (CH), 57.4 (CH_2), 54.7 (CH), 51.8 (CH_2), 34.0 (CH_2), 27.1 (CH_3), 23.0 (CH_2), 22.4 (CH_3), 20.2 (CH_3), 19.2 (C_q). LCMS: *m/z* 634.2 [MH$^+$].

Synthesis of 2*S*,3*R*,5*S*-4-{[2-*tert*-Butoxycarbonyl-2-(2,4,6-trimethylbenzenesulfonylamino)ethylcarbamoyl]methoxy}-2-formylpyrrolidine-1-carboxylic Acid Benzyl Ester (11). 10 (120 mg, 0.19 mmol) and 293 μL (2.1 mmol) of NEt_3 were dissolved in 2 mL of DCM/DMSO (v/v = 3/1) and cooled to 0 °C. SO_3−pyridine complex (302 mg, 1.9 mmol) was added and the reaction mixture was stirred for 2 h. DCM was removed by an evaporator and the crude reaction mixture was poured into 30 mL of ethyl acetate. The organic layer was extracted with H_2O, saturated $NaHCO_3$, and NaCl solution. The organic layer was dried over Na_2SO_4 and the solvent was removed by an evaporator. Yield: 109 mg (91%). ^{1}H NMR (DMSO-d_6): δ = 9.42 (s, 1H), 8.06 (d, 1H, J = 8.8), 7.79 (t, 2H, J = 5.8), 7.35 (m, 5H), 6.97 (s, 2H), 5.10 (m, 2H), 4.21 (m, 1H), 4.10 (m, 1H), 3.85−3.46 (m, 5H), 3.41 (m, 1H), 3.34 (t, 2H, J = 11.7), 3.18 (m, 1H), 2.53 (s, 6H), 2.21 (s, 3H), 1.12(s, 9H). LCMS: *m/z* 632.6 [MH$^+$].

Synthesis of 2*S*,3*R*,5*S*-4-{[2-Carboxy-2-(2,4,6-trimethylbenzenesulfonylamino)ethylcarbamoyl]methoxy}-2-[(4-chloropyridin-2-ylamino)methyl]pyrrolidine-1-carboxylic Acid Benzyl Ester (12b). 11 (40 mg, 0.063 mmol), 16.3 mg (0.127 mmol) of 4-chloropyridin-2-ylamine, and 37.8 μL (0.127 mmol) of $Ti(OiPr)_4$ were dissolved in 500 μL of dichloroethane. After stirring for 4 h at room temperature, 27.9 mg (0.444 mmol) of $NaBH(OAc)_3$ was added and the reaction was stirred overnight. Saturated $NaHCO_3$ solution (100 μL) was added, and the mixture was stirred for 1 h and dried with Na_2SO_4. The solvent was evaporated and the crude reaction mixture was redissolved in 300 μL of TFA and stirred for 2 h at room temperature. After evaporation of the TFA, the product was purified by HPLC and freeze-dried with ACN/H_2O. Yield: 11.6 mg (23% TFA salt). ^{1}H NMR (DMSO-d_6): δ = 7.95 (dd, 1H, J = 6.6, J = 12.4), 7.90 (d, 1H, J = 6.6), 7.67 (m, 1H), 7.35 (m, 5H), 6.95 (s, 2H), 6.77 (m, 1H), 5.09 (s, 2H), 4.13 (m, 2H), 4.06 (m, 1H), 3.82 (m, 2H), 3.74−3.57 (m, 4H), 3.53−3.33 (m, 4H), 3.15 (m, 1H), 2.51 (s, 6H), 2.21 (s, 3H), 2.12 (m, 1H), 1.90 (m, 1H). LCMS: *m/z* 689.2 [MH$^+$].

General Procedure for the Synthesis of Compounds 1, 19a−d. The compounds were purified by HPLC with >98% purity (10−20 mg). The corresponding overall yields were between 15 and 55%.

Synthesis of 12*S*,14*R*,30*S*-4-{[2-Carboxy-2-(2,4,6-trimethylbenzenesulfonylamino)ethylcarbamoyl]methoxy}-2-(pyridin-2-ylaminomethyl)pyrrolidine-1-carboxylic Acid Benzyl Ester (1).4 (17 mg, 40 μmol), 14 mg (0.0409 mmol) of **5**, 20 mg (41 μmol) of HBTU, and 16 mL (120 μmol) of DIPEA were dissolved in 2 mL of DMF and stirred for 2 h. The solvent was removed by an evaporator and the crude product was purified by HPLC. The product was dissolved in 2 mL of TFA and the mixture stirred for 2 h at room temperature. After evaporation of the TFA, the crude product was freeze-dried using ACN/H_2O. Yield: 14.4 mg (47%, TFA salt). ^{1}H NMR (DMSO-d_6): δ = 8.59 (s, broad, 1H) 7.94 (d, 1H, J = 8.8), 7.94 (s, broad, 1H), 7.70 (t, 1H, J = 5.8), 7.35 (s, broad, 3H), 7.31 (s, broad, 2H), 7.11 (d, 1H, J = 9.2), 6.96 (s, 2H), 6.92−6.76 (m, 2H), 5.09 (s, 2H), 5.02 (t, 1H, J = 12.2), 4.11 (s, broad, 2H), 3.88−3.35 (m, 8H) 2.52 (s, 6H), 2.22 (s, 3H), 1.89 (m, 1H). ^{13}C NMR (DMSO-d_6): δ = 171.2 (C_q), 169.2 (C_q), 153.3 (C_q), 141.3 (C_q), 138.4 (C_q), 136.7 (C_q), 134.5 (C_q), 131.4 (CH), 128.4 (CH), 127.8 (CH), 127.5 (CH), 112.1 (CH), 77.2 (CH), 73.2

(CH_2), 67.5 (CH_2), 66.4 (CH_2), 66.1 (CH_2), 55.0 (CH), 54.3 (CH), 51.6 (CH_2), 44.0 (CH_2), 22.5 (CH_3), 20.3 (CH_3). LCMS: *m/z* 654.6 [MH^+].

General Procedure for the Synthesis of the Diaminopropionic Acid Derivatives 17 and 18. Synthesis of 3*S*-3-Amino-2-[(1-methylcyclohexanecarbonyl)amino]propionic Acid *tert*-Butyl Ester (18). 1-Methylcyclohexanecarboxylic acid (6.53 g, 45 mmol), 300 mg (1.9 mmol) of 4-pyrrolidinopyridine, 16.9 mL (115 mmol) of DIPEA, and 17.4 g (45.9 mmol) of HBTU were dissolved in 60 mL of DCM and stirred for 10 min. L-H-Asn-OtBu (**21**) (7.2 g, 38.3 mmol) was added and the reaction mixture was stirred at room temperature for 5 h. The solvent was removed by an evaporator. The crude reaction mixture was dissolved in 250 mL of ethyl acetate and washed with 100 mL of water. The organic layer was dried over Na_2SO_4 and the solvent was removed by an evaporator. The product was dissolved in DCM and diethyl ether, and a white solid was filtered off. After removal of the solvent, the product was recrystallized from ethyl acetate/hexane. Yield: 9.37 g (78%).

The coupling product (9.37 g, 30 mmol) was dissolved in 140 mL of acetonitrile and 70 mL of water and cooled to 0 °C. PIFA (14.2 g, 33 mmol) was added and the reaction mixture was stirred for 10 min. Dry pyridine (4.83 mL, 60 mmol) was added and the solution was stirred overnight. Acetonitrile was removed in vacuo and the aqueous layer was acidified with 1 M HCl (25 mL). After addition of 200 mL of water, the aqueous layer was extracted with 400 mL of diethyl ether. The organic layer was extracted three times with 25 mL of 1 M HCl. The combined aqueous layers were neutralized with $NaHCO_3$ (solid) and extracted three times with 300 mL of ethyl acetate. The combined organic layers were dried over Na_2SO_4, and the solvent was removed under reduced pressure. The product was purified by column chromatography on silica gel using ethyl acetate/hexane. Yield: 7.2 g (84%). ^{1}H NMR (DMSO-d_6): $\delta = 7.58$ (d, 1H, $J = 7.3$), 4.14 (m, 1H), 2.94 (dd, 1H, $J = 5.1$, $J = 13.2$), 2.83 (dd, 1H, $J = 7.3$, $J = 13.2$), 1.99 (s, 1H), 1.97 (s, 1H), 1.50−1.12 (m, 10H), 1.38 (s, 9H), 1.06 (s, 3H). ^{13}C NMR (DMSO-d_6): $\delta = 176.7$ (C_q), 170.1 (C_q), 80.4 (C_q), 54.9 (CH), 41.9 (C_q), 41.8 (C_q), 35.1 (CH_2), 34.9 (CH_2), 27.6 (CH_3), 26.8 (CH_3), 25.3 (CH_2), 22.6 (CH_2), 22.5 (CH_2). LCMS: *m/z* 285.2 [MH^+].

Integrin Binding Assays. Solid-Phase Binding Assay. The inhibiting activity and integrin selectivity of the integrin inhibitor were determined in a solid-phase binding assay using soluble integrins and coated extracellular matrix protein. Binding of integrins was then detected by specific antibodies in an enzyme-linked immunosorbant assay (ELISA). Fibronectin, vitronectin, and laminin were purchased from Sigma, and fibrinogen was from Calbiochem (EMD Biosciences, Darmstadt, Germany). The integrin α5β1 extracellular domain Fc-fusion was a generous gift from M. Humphries and expressed and purified as described by Coe et al.[18] Integrins αvβ3, αvβ5, and α3β1 were purchased from Chemicon (Chemicon Europe) and αIIbβ3 from Kordia (Kordia Life Science, Leiden, The Netherlands). The integrin antibodies were purchased from Pharmingen, BD Bioscience Europe (αvβ3 and αIIbβ3), Chemicon (αvβ5, α3β1), and Sigma (anti-human−Fc−horse radish peroxidase (HRP) antibody conjugate, anti-mouse−HRP conjugate, anti-rabbit−HRP conjugate). The detection of HRP was performed using HRP substrate solution 3,3,5,5′-tetramethylethylenediamine (TMB, Seramun, Germany) and 1 M H_2SO_4 for stopping the reaction. The absorbance was measured at 450 nm with a SpectraMax Plus reader (Molecular Devices). The resulting inhibition curves were analyzed using SoftMaxPro 4.0 software, and the turning point depicts the IC_{50} value.

Integrin α5β1: Nunc-Immuno maxisorp plates (Nalge Nunc Europe Ltd) were coated overnight at 4 °C with fibronectin (0.25 μg/mL) in 15 mM Na_2CO_3, 35 mM $NaHCO_3$, pH 9.6. All subsequent washing and binding steps were performed in 25 mM Tris, pH 7.6, 150 mM NaCl, 1 mM $MnCl_2$, 1 mg/mL BSA. The plates were blocked with 3% BSA in PBS 0.1% Tween 20 for 1 h at room temperature. Soluble integrin α5β1 (0.5 μg/mL) and a serial dilution of integrin inhibitor were incubated in the coated wells for 1 h at room temperature. The detection antibody (anti-human−Fc−HRP antibody conjugate) was then applied for 1 h at room temperature and binding was visualized as described above. For the αvβ3 assay, plates were coated with vitronectin (1 μg/mL) and blocked as described for α5β1. Soluble αvβ3 (1 μg/mL) was incubated with a serial dilution of integrin inhibitor for 1 h at room temperature. Primary (anti-αvβ3) and secondary antibody (anti-mouse−HRP conjugate) were applied for 1 h at room temperature, and binding was visualized as described above. For the αvβ5 assay, plates were coated with vitronectin (5 μg/mL) and blocked as described for α5β1. Soluble αvβ5 (1.5 μg/mL) was incubated with a serial dilution of integrin inhibitor (25 mM Tris, pH 7.6, 150 mM NaCl, 1 mM $MnCl_2$, 1 mM $MgCl_2$, 1 mM $CaCl_2$, 1 mg/mL BSA, 0.05% Tween20) for 1 h at room temperature. Primary (anti-αvβ5) and secondary antibody (anti-mouse−HRP conjugate) were applied for 1 h at room temperature, and binding was visualized as described above. For the αIIbβ3 assay, plates were coated with fibrinogen (10 μg/mL) and blocked as described for α5β1. Soluble αIIbβ3 (5 μg/mL) was incubated with a serial dilution of integrin inhibitor (25 mM Tris, pH 7.6, 150 mM NaCl, 1 mM $MnCl_2$, 1 mg/mL BSA 1 mM $MgCl_2$, 1 mM $CaCl_2$) for 1 h at room temperature. Primary (anti-CD41b) and secondary antibody (anti-mouse-HRP conjugate) were applied for 1 h at room temperature, and binding was visualized as described above. For the α3β1 assay, plates were coated with laminin (5 μg/mL) and blocked as described for α5β1. Soluble α3β1 (2 μg/mL) was incubated with a serial dilution of integrin inhibitor (25 mM Tris, pH 7.6, 150 mM NaCl, 1 mM $MnCl_2$, 1 mg/mL BSA, 0.05% Tween20) for 1 h at room temperature. Primary (α3β1, polyclonal) and secondary antibody (anti-rabbit−HRP conjugate) were applied for 1 h at room temperature, and binding was visualized as described above.

Acknowledgment. We thank Edith Weigt, Frank Polster, Seike Gericke, and Thorsten Lanz for technical assistance and Dr. Ulrich Reineke and Dr. Gerd Hummel for proofreading the manuscript.

Supporting Information Available: Experimental procedures for microsome stability assay and cell-based assay; analytical data and experimental procedures for the compounds **12a**, **16a**−**c**, **19a**, **19c**−**k** and **17**; table of purity and HPLC analysis for the target compounds **1**, **7a**−**e**, **12a**−**c**, and **19a**−**k**. This material is available free of charge via the Internet at http://pubs.acs.org.

References

(1) Hynes, R. O. Integrins: Bidirectional, allosteric signaling machines. *Cell* **2002**, *110*, 673−687.
(2) Humphries, J. D.; Byron, A.; Humphries, M. J. Integrin ligands at a Glance *J. Cell Sci.* **2006**, *119*, 3901−3903.
(3) Francis, S. E.; Goh, K. L.; Hodivala-Dilke, K.; Bader, B. L.; Stark, M.; Davidson, D.; Hynes, R. O. Central roles of α5β1 integrin and fibronectin in vascular development in mouse embryos and embryoid bodies. *Arterioscler. Thromb. Vasc. Biol.* **2002**, *22*, 927−933.
(4) Kim, S.; Bell, K.; Mousa, S. A.; Varner, J. A. Regulation of angiogenesis in vivo by ligation of integrin α5β1 with the central cell-binding domain of fibronectin. *Am. J. Pathol.* **2000**, *156*, 1345−1362.
(5) Umeda, N.; Kachi, S.; Akiyama, H.; Zahn, G.; Vossmeyer, D.; Stragies, R.; Campochiaro, P. A. Suppression and regression of choroidal neovascularization by systemic administration of an α5β1 integrin antagonist. *Mol. Pharmacol.* **2006**, *69*, 1820−1828.
(6) Parsons-Wingerter, P.; Kasman, I. M.; Norberg, S.; Magnussen, A.; Zanivan, S.; Rissone, A.; Baluk, P.; Favre, C. J.; Jeffry, U.; Murray, R.; McDonald, D. M. Uniform overexpression and rapid accessibility of α5β1 integrin on blood vessels in tumors. *Am. J. Pathol.* **2005**, *167*, 193−211.
(7) Xiong, J. P.; Stehle, T.; Zhang, R.; Joachimiak, A.; Frech, M.; Goodman, S. L.; Arnaout, M. A. Crystal structure of the extracellular segment of integrin αVβ3 in complex with an Arg-Gly-Asp ligand. *Science* **2002**, *296*, 151−155.
(8) Marinelli, L.; Meyer, A.; Heckmann, D.; Lavecchia, A.; Novellino, E.; Kessler, H. Ligand binding analysis for human α5β1 integrin: Strategies for designing new α5β1 integrin antagonists. *J. Med. Chem.* **2005**, *48*, 4204−4207.
(9) Pitts, W. J.; Wityak, J.; Smallheer, J. M.; Tobin, A. E.; Jetter, J. W.; Buynitsky, J. S.; Harlow, P. P.; Solomon, K. A., Corjay, M. H.; Mousa, S. A.; Wexler, R. R.; Jadhav, P. K. Isoxazolines as potent antagonists of the integrin αvβ3. *J. Med. Chem.* **2000**, *43*, 27−40.

(10) Radhakrishna, A. S.; Parham, M. E.; Riggs, R. M.; Loudon, G. M. New method for direct conversion of amides to amines. *J. Org. Chem.* **1979**, *44*, 1746−1747.
(11) Searle, M. S.; Williams, D. H.; Gerhard, U. Partitioning of free energy contributions in the estimation of binding constants: Residual motions and consequences for amide−amide hydrogen bond strengths. *J. Am. Chem. Soc.* **1992**, *114*, 10697−10704.
(12) Baldauf, C.; Günther, R.; Hoffmann, H.-J. Conformational properties of sulfonamido peptides. *J. Mol. Struct. (Theochem*) **2004**, *675*, 19−28.
(13) Muether, P. S.; Dell, S.; Kociok, N.; Stragies, R.; Zahn, G.; Kirchhof, B.; Joussen, A. M. Integrin α5β1-inhibiting small molecule reduces corneal neovascularisation. *Exp. Eye Res.* **2007**, in press.
(14) Zahn, G.; Stragies, R.; Wills, M.; Birkner, S.; Knolle, J. Evaluation of a small molecule α5β1 integrin antagonist for ocular neovascularization in a laser induced CNV model in monkey, *ARVO Annu. Meeting Abstr.* **2005**, 4169.
(15) Dietrich, T.; Onderka, J.; Bock, F.; Kruse, F. E.; Vossmeyer, D.; Stragies, R.; Zahn, G.; Cursiefen, C. Selective inhibition of lymphangiogenesis by integrin. α5 blockade−Functional role of integrins in lymphangiogenesis, *J. Am. Path.* **2007**, May 24; [Epub ahead of print].
(16) Labute, P.; Williams, C.; Feher, M.; Sourial, E.; Schmidt, J. M. Flexible alignment of small molecules. *J. Med. Chem.* **2001**, *44*, 1483−1490.
(17) Halgren, T. A. The Merck molecular force field. I. Basis, form, scope, parametrization, and performance of MMFF94. *J. Comput. Chem.* **1996**, *17*, 490−519.
(18) Coe, A. P.; Askari, J. A.; Kline, A. D.; Robinson, M. K.; Kirby, H.; Stephens, P. E.; Humphries, M. J. Generation of a minimal α5β1 integrin-Fc fragment. *J. Biol. Chem.* **2001**, *276*, 35854−66.

JM070002V